Applied Surface Science 255 (2009) 4334–4340

Contents lists available at ScienceDirect

Applied Surface Science

journal homepage: www.elsevier.com/locate/apsusc

Nanomaterials based upon silylated layered double hydroxides

Qi Tao [a,b,c], Hongping He [a,b,*], Ray L. Frost [b,**], Peng Yuan [a], Jianxi Zhu [a]

[a] Guangzhou Institute of Geochemistry, Chinese Academy of Sciences, Guangzhou 510640, PR China
[b] Inorganic Materials Research Program, School of Physical and Chemical Sciences, Queensland University of Technology, GPO Box 2434, Brisbane, Queensland 4001, Australia
[c] Graduate School of Chinese Academy of Sciences, Beijing 100039, PR China

ARTICLE INFO

Article history:
Received 2 October 2008
Received in revised form 12 November 2008
Accepted 13 November 2008
Available online 21 November 2008

Keywords:
Layered double hydroxide
Hydrotalcite
Anionic surfactant
Silylation
Surface properties
TEM
FTIR
TG

ABSTRACT

A class of nanomaterials based upon the surface modification of layered double hydroxides (LDHs) have been synthesized by grafting silanes onto the surfaces of the LDH. By in situ coprecipitation, the surfaces of a LDH have been modified through grafting of 3-aminopropyltriethoxysilane (APTS) using the anionic surfactant Na-dodecylsulfonate (SDS). The synthesized nanomaterials were characterized by X-ray diffraction (XRD), attenuated total reflection Fourier-transform infrared spectroscopy (ATR FTIR), thermogravimetry (TG) and transmission electron microscopy (TEM). The grafted LDH (LDH-G) displays distinct XRD patterns proving the obtained materials are a new and different phase. The FTIR spectra of the silylated hydrotalcite show bands attributed to Si–O–M (M = Mg and Al) vibration at 996 cm^{-1}, suggesting that APTS has successfully been grafted onto the LDH layers. The TG curves prove the grafted sample has less M–OH concentration and less interlayer water molecules, as indicated by the M–OH consumption during the condensation reaction between Si–OH and M–OH on the LDH surface. The grafted sample displays a ribbon-like thin sheet in the TEM images, with the lateral thickness estimated as 2.5 nm.

1. Introduction

Grafting, which is one of the most useful methods of introducing functional groups onto the surfaces of inorganic compounds, has aroused considerable interest of researchers [1–5]. Among these methods, silylation is the most common way to modify the physical and chemical properties of the surface. Organosilane grafts onto the silanol groups "populated" surface, as a part of the walls or trapped within the interlayers, permits a precise control over the surface component and pore features for specific applications, and at the same time stabilizing the materials against hydrolysis. The products of such chemistry form the basis of novel inorganic–organic hybrid materials, in which the inorganic parts provide mechanical, thermal, and structural stability, whereas the organic parts can change the flexibility of the framework, optical properties, hydrophilicity and hydrophobicity of the solid [6].

Layered double hydroxides (LDHs), also known as hydrotalcite compounds, are the only clay with positively charged layers with the surface charges balanced by interlayer anions. LDHs are commonly expressed as $[M_{1-x}^{2+}M_x^{3+}(OH)_2]^{x+}A_{x/n}^{n-}\cdot mH_2O$, where M^{2+} and M^{3+} are divalent and trivalent cations that occupy octahedral positions in the hydroxide layers, A^{n-} is an interlayer anion and x is defined as the $M^{3+}/(M^{2+} + M^{3+})$ ratio. The excellent anionic exchange capacity makes these materials suitable for adsorbents, ion exchangers, pharmaceutics, catalysts or catalyst supports, etc. [7–13]. There are many studies on the modification of the surfaces of cationic clays, for example, smectite group minerals and minerals from the serpentine group [14–16]. There are also studies reported on grafting the other organo functional groups to the surface of LDHs [17–22]. However, very limited attention [23,24] has been paid to the grafting of silanes on to the surface of layered double hydroxides. The most important reason lies in their higher surface charge density (about one positive charge per 25 $Å^2$ for the case of $x = 0.32$) [25] compared with other clays (e.g. the unit cell charge of smectite clays varied from −0.6 to −1.4 per O_{20} unit) [26]. In order to overcome such a problem, researchers try to use anions with long alkyl chain to enlarge the interlayer distance of LDHs. These reactions enable the formation of positive nano-scale single layers through by using dodecylsulfate anions in organic polar solvents as described earlier [27–30]. These large anions not only enlarge the interlayer space but also introduce the solvent molecules into the interlayer and thus decrease the interaction between the layers. As a result, the layer structure of the synthesized organo-LDHs materials are exfoliated

* Corresponding author at: Inorganic Materials Research Program, School of Physical and Chemical Sciences, Queensland University of Technology, GPO Box 2434, Brisbane, Queensland 4001, Australia.
** Corresponding author. Tel.: +61 7 3138 2407; fax: +61 7 3138 1804.
E-mail addresses: hehp@gig.ac.cn (H. He), r.frost@qut.edu.au (R.L. Frost).

0169-4332/$ – see front matter © 2008 Elsevier B.V. All rights reserved.
doi:10.1016/j.apsusc.2008.11.030

and form single layer suspension. This methodology provides a new mechanism for the grafting of LDHs with functional groups. Methodology to synthesize 3-aminopropyltriethoxysilane (APTS) modified LDH was only found very recently [22–24]. The dodecylsulfate anion interlayered LDH was prepared firstly, followed by reaction with APTS in organic solvents. The centryltrimethylammonium bromide (CTAB) was also used to precipitate the dodecylsulfate anions. However, the problem is that the Br^- has to be maintained in the interlayer of the resultant materials for charge balance.

In this research we here present a one-step method for the in situ grafting of APTS onto the surface of LDHs in aqueous solution [6]. In this way, a new and novel class of nanomaterials have been produced. The grafted LDHs have been synthesized by coprecipitation in the presence of Na-dodecylsulfonate (SDS) and APTS. The structure and properties of the as-synthesized materials were characterized by X-ray diffraction (XRD), attenuated total reflection Fourier-transform infrared spectroscopy (ATR FTIR), thermogravimetry (TG) and transmission electron microscopy (TEM). The effects of SDS and APTS to the resultants were discussed in terms of the geometrical arrangements, spectroscopy, the thermal properties and morphology.

2. Experimental

2.1. Synthesis of materials

2.1.1. $Mg_6Al_2(OH)_{16}CO_3{\cdot}4H_2O$ (LDH)

The hydrotalcites were prepared by coprecipitation [31]. About 9.6 g of $Mg(NO_3)_2{\cdot}6H_2O$ and 4.7 g of $Al(NO_3)_3{\cdot}9H_2O$ with a molar ratio of 3:1 (Mg^{2+}/Al^{3+}) were dissolved in 44 cm^3 distilled water (Solution A). About 4 g NaOH were dissolved in 50 cm^3 of distilled water (Solution B). At room temperature, Solution B and Solution A were dropped into 50 cm^3 distilled water with vigorous stirring. The pH value of the mixture was kept at 10 pH units. The mixture was aged at 80 °C for 12 h. The resultant precipitate was filtered, washed with distilled water, and dried at 80 °C. The obtained material was denoted as LDH.

2.1.2. LDH–SDS–APTS (LDH-G)

19.2 g of $Mg(NO_3)_2{\cdot}6H_2O$ and 9.4 g of $Al(NO_3)_3{\cdot}9H_2O$ with a molar ratio of 3:1 (Mg^{2+}/Al^{3+}) were dissolved in 90 cm^3 of distilled water (Solution C). ~8 g NaOH and 6.8 g Na-dodecylsulfonate (SDS) were dissolved in 50 cm^3 distilled water (Solution D). 5.0 cm^3 APTS was dissolved in 50 cm^3 ethanol (Solution E). At room temperature, Solutions C, D and E were added to 100 cm^3 distilled water with vigorous stirring, maintaining the pH value of the mixture at ~10 pH units. The mixture was aged at 80 °C in a water bath for about 12 h, and afterwards, the resultant slurry was filtered, washed with distilled water, and dried at 80 °C. The obtained material was denoted as LDH-G.

2.1.3. LDH–SDS (LDH-S)

The only anionic surfactant modified layered double hydroxide was synthesized following the procedure as for LDH-G, except for the absence of the organosilane. The obtained material was denoted as LDH-S.

2.2. Characterization of materials

2.2.1. X-ray-diffraction

Powder XRD patterns were recorded using a Philips PANalytical X'Pert PRO X-ray diffractometer (radius: 240.0 mm). Incident X-ray radiation was produced from a line focused PW 3373/10 Cu X-ray tube, operating at 40 kV and 40 mA, providing a $K\alpha_1$ wavelength of 1.5418 Å. The incident beam was monochromated through a 0.020-mm Ni filter then passed through a 0.04 rad. Soller slit a 15 mm fixed mask with 0.25° divergence slit, 0.5° anti-scatter slit, between 9 and 65° (2θ) at a step size of 0.0167°. For XRD at low angle section, it was between 2 and 10° (2θ) at a step size of 0.0167° with variable divergence slit and 0.125° anti-scatter slit.

2.2.2. Infrared spectroscopy

Infrared spectra were obtained using a Nicolet Nexus 870 FTIR spectrometer with a smart endurance single bounce diamond ATR cell. Spectra over the 4000–525 cm^{-1} range were obtained by the co-addition of 64 scans with a resolution of 4 cm^{-1} and a mirror velocity of 0.6329 cm s^{-1}.

Spectroscopic manipulation, such as baseline adjustment, smoothing and normalisation were performed using the Spectracalc software package GRAMS (Galactic Industries Corporation, NH, USA). Band component analysis was undertaken using the Jandel 'Peakfit' software package, which enabled the type of fitting function to be selected and allows specific parameters to be fixed or varied accordingly. Band fitting was done using a Gauss–Lorentz, cross-product function with the minimum number of component bands used for the fitting process. The Gauss–Lorentz ratio was maintained at values greater than 0.7 and fitting was undertaken until reproducible results were obtained with squared correlations (r^2) greater than 0.995.

2.2.3. Thermal analysis

Thermogravimetry of samples were recorded on a SDT Q600 thermobalance (TA, USA) between 25 and 1000 °C with a heating ratio of 10 °C min^{-1} under N_2 atmosphere (100 ml min^{-1}).

2.2.4. Transmission electron microscopy

Transmission electron microscopy images were obtained in a Philips CM120 electron microscope operating at an acceleration voltage of 120 kV. The specimens for TEM observation were prepared by the following procedure. The clay sample was ultrasonically dispersed in ethanol for 5 min, and then a drop of sample suspension was dropped onto a carbon-coated copper grid, which was left to stand for 10 min and transferred into the microscope.

2.2.5. Composition analyses

The composition of Mg, Al and Si were determined by volumetric method analyses. For the content of Si, alkali fusion method was adopted to fuse the samples in KOH. The content of K_2SiO_3 resulted from Si in the sample are determined by volumetric method. For the content of Mg and Al, HF was used to separate SiF_4, and then the Mg and Al concentrations in solution was analysed by titrimetric methods.

3. Results and discussion

3.1. XRD results

Powder X-ray diffraction is a very powerful technique for characterizing the structure of materials. The d value of layered materials, which reflects the framework of the interlayer, can be calculated directly from the diffraction angles through Bragg's law. The XRD patterns of LDH, LDH-S and LDH-G at 2θ = 2–10° and 8–65° are shown in Figs. 1 and 2, respectively. The XRD patterns of LDH (Figs. 1a and 2a) show a typical and well-ordered layer structure with a basal spacing ($d_{0\,0\,3}$) of 7.9 Å [32]. The d value is slightly larger than that of the calculated value (about 7.8 Å), caused by the interlayer anion (NO_3^-).

The XRD diffraction patterns of LDH-S are displayed in Figs. 1b and 2b. Compared with the XRD patterns for LDH, a new series of

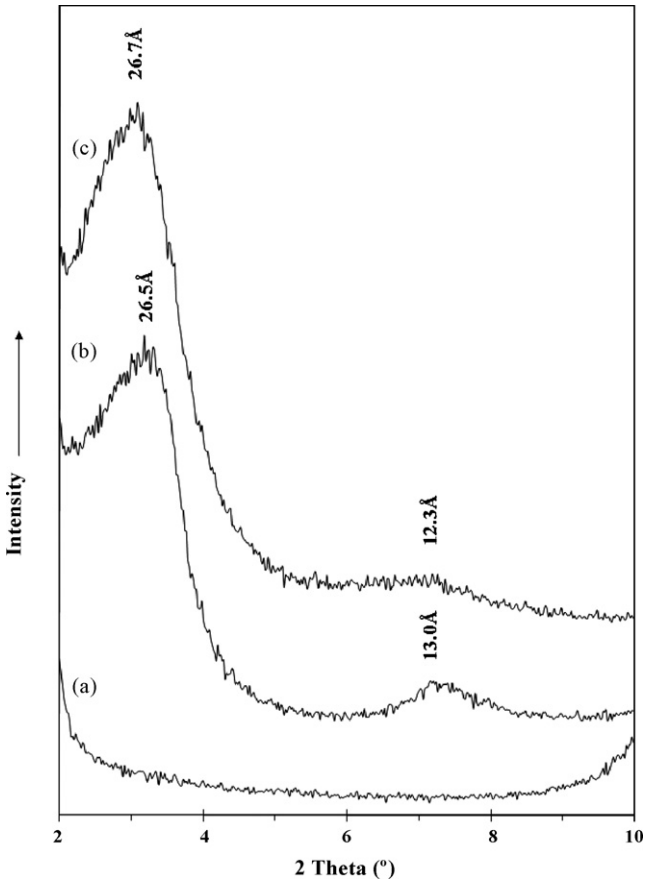

Fig. 1. Powder X-ray diffraction patterns of the resultants in the 2θ 2–10° region: (a) LDH, (b) LDH-S and (c) LDH-G.

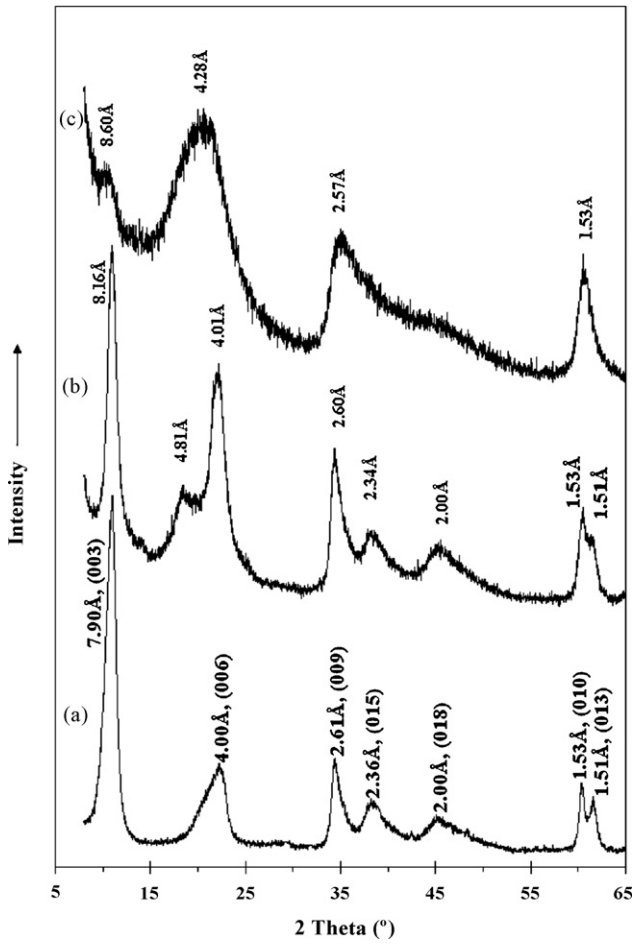

Fig. 2. Powder X-ray diffraction patterns of the resultants in the 2θ 5–65° region: (a) LDH, (b) LDH-S and (c) LDH-G.

peaks is clearly shown at lower diffraction angles (2θ = 2–10°) with *d* values of 26.5 and 13.0 Å. The expanded basal spacings, compared with that of LDH, suggest that the anionic surfactants have been intercalated into LDH interlayer spaces [33,34], similar to those reported for cationic surfactant modified montmorillonites [35,36]. The basal spacing of LDH-S is the sum of the interlayer height and the thickness of a Al/Mg-hydroxide sheet (about 4.8 Å) [23]. In this case, the basal spacing of 26.5 Å is larger than the sum of the thickness of a Al/Mg-hydroxide sheet (ca. 4.8 Å) and the length of alkyl chain of DS^- anion (ca. 20.8 Å) suggesting that the intercalated surfactants adopt a paraffin bilayer arrangement model [37,38]. The broad and weak peak at ca. 13° may be the (0 0 2) reflection, corresponding to the basal spacing of 26.5 Å. The large interlayer distance indicates the newly formed structure has less attraction between the layer and the interlayer anions, although the *d* value of LDHs can also vary according to the ratio of M^{2+}/M^{3+}. The similar results is report by Clearfield et al. [39]. They proved the sulfate anions are perpendicular to the LDHs layer with the chains in an all-*trans* conformation in their study. Also, it can be found that the pristine LDH structure is partly preserved as indicated by the series reflections at 8.16 (0 0 3), 4.01 (0 0 6), 2.60 (0 0 9), 2.34 (0 1 5) and 2.00 Å (0 1 8) (Fig. 2b).

The *d* values of the diffraction patterns at 2θ = 2–10° of LDH-G are 26.74 and 12.31 Å, respectively (Fig. 1c). These *d* values are only slightly different from those of LDH-G. However, the compositional analysis of the LDH-G, obtained by chemical titration analysis, shows that the molar ratios of Al/Si and Mg/Al in LDH-G are about 2.29 and 3.24, respectively. This indicates that silane has been successfully loaded onto the obtained materials. A slight increase of Mg/Al ratio in LDH-G, compared with that deduced from the added reactants, may be resulted from the dissolution of Al from the LDH crystals during the grafting procedure as reported in literature [40]. Here, it can be found that the presence of APTS (the length is about 7 Å [41]) has little influence on the interlayer gallery height. The silane (APTS)-loaded condensate with the –OH units on the LDH surface may not be covered by the surfactant DS^-. The silane may also react with the OH units of the broken edges of the plates. The similar results can be found in the silane grafting study on Laponite [42].

In Fig. 2b and c, both the decrease of peak intensity and the broadening of diffraction peaks' width suggest the lower crystallinity of LDH-G than LDH and LDH-S. In the 2θ range of 10–30°, it can be found that the (0 0 6) diffraction of pristine LDH was replaced by a broad peak. This is explained as an evidence of the exfoliation process by previous study [24]. The reflections corresponding to LDH becomes very weak, indicating that grafting silane onto LDH have a significant influence on the layered structure of the resulting materials. This is also evidenced by FTIR and TG results as discussed in the following parts. The single sheets restack with hydrolysed APTS and DS^- alternately to form a new and more orderly sequences stacking matrices [43]. This evidence is supported by the morphological difference observed from TEM images.

3.2. FTIR spectroscopy

The FTIR spectra of LDH, LDH-S and LDH-G are presented in Fig. 3 (3750–2750 cm^{-1}), Fig. 4 (1700–500 cm^{-1}), and Fig. 5 (1100–960 cm^{-1}), respectively. For LDH (Fig. 3a), the O–H-related bands

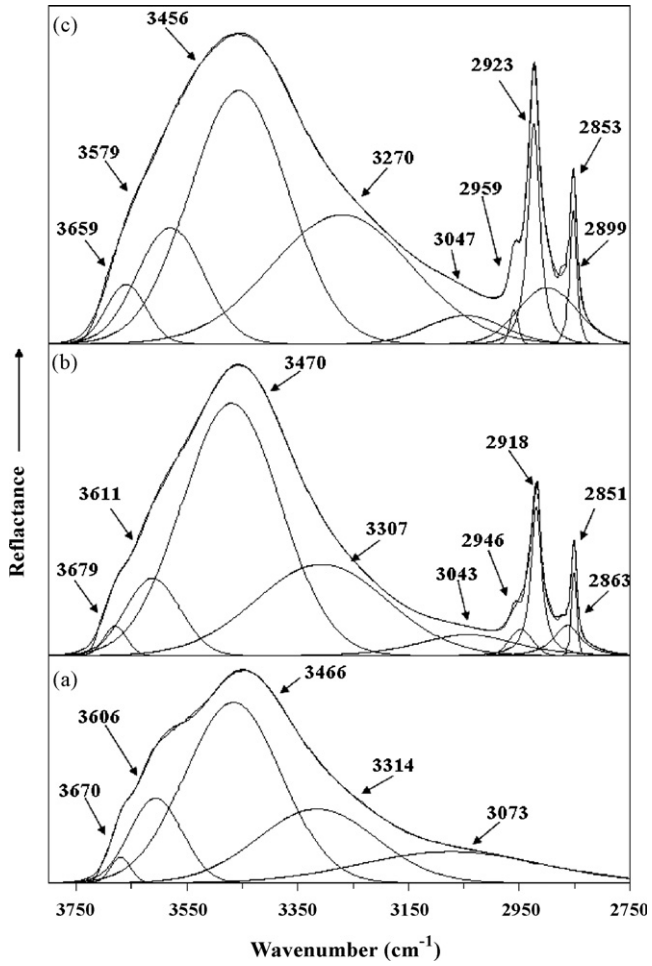

Fig. 3. FTIR spectra of the resultants in the 3750–2750 cm^{-1} region: (a) LDH, (b) LDH-S and (c) LDH-G.

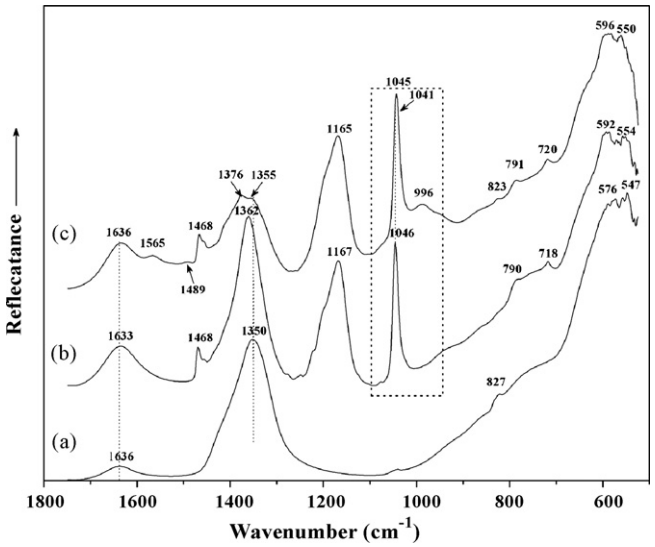

Fig. 4. FTIR spectra of the resultants in the 1700–500 cm^{-1} region: (a) LDH, (b) LDH-S and (c) LDH-G.

are at around 3466 (absorbed water), 3606 and 3670 (stretching modes of M–OH), 3314 (H-bonds between –OH and interlayer water) and 3073 cm^{-1} (the bridge bond between H_2O and anions) [44]. Another band corresponding to water bending mode is observed at ~1636 cm^{-1} (Fig. 4a). The strong and sharp band at ~1350 cm^{-1} is due to the ν_3 antisymmetric stretching mode of CO_3^{2-} and the 827 cm^{-1} band is assigned to ν_2 modes of the CO_3^{2-} located within interlayer spaces. The bands at 576 and 547 cm^{-1} are attributed to the M–O stretching vibration (M = Mg^{2+}, Al^{3+}).

The spectroscopy of LDH-S (Figs. 3b and 4b) is more informative. In addition to the all bands at 3043–3679, 1633, 592 and 547 cm^{-1} corresponding to the hydroxide layer, it also shows C–H and S–O bands due to SDS. The C–H bands are centred at 2918 and 2851 cm^{-1} with small shoulders at 2946 and 2863 cm^{-1} (stretching), and the bending mode at 1468 cm^{-1}. The S–O and S=O stretching modes of DS^- are located at 1167 (Fig. 4b), 1046 and 1036 cm^{-1} (Fig. 5a). The bands at 790 and 718 cm^{-1} are ascribed to C–S–O and O–S–O bending vibrations of DS^-. The band located at 1360 cm^{-1} corresponds to the CO_3^{2-} antisymmetric stretching vibration which remained from the unreacted LDH as indicated by the XRD patterns.

The spectroscopy of LDH-G (Figs. 3c, 4c and 5b) is different from that of LDH-S. Grafting APTS onto LDH brings a group of new bands at 3270 ($-NH_2$ stretching), 1565, 1489 ($-NH_2$ scissoring), 1376 ($-CH_2-$ twisting), 1041 (Si–O–C asymmetric stretching) [45] and 996 cm^{-1} (Figs. 4c and 5b). The occurrence of Si–O–M (M = Mg and Al) vibration at 996 cm^{-1} strongly suggests that APTS has successfully been grafted onto LDH. Meanwhile, the O–H-related bands obviously shift to the lower wavenumber. In LDH-S, these bands shift to a slightly higher wavenumber, due to the effect of the surfactant change the surface property from hydrophilicity to hydrophobicity [6]. However, silane grafting takes a significant influence on the vibration wavenumber shift of O–H vibration to a lower wavenumber, resulting from the hydroxyl consumption during the condensation between LDH and silane A previous study

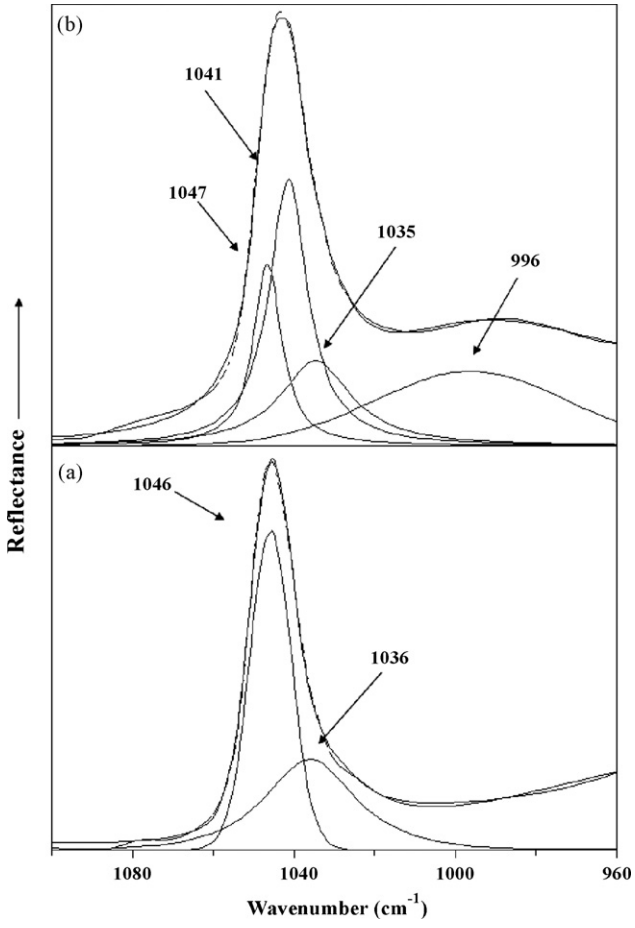

Fig. 5. FTIR spectra in the 1100–960 cm^{-1} region: (a) LDH-S and (b) LDH-G.

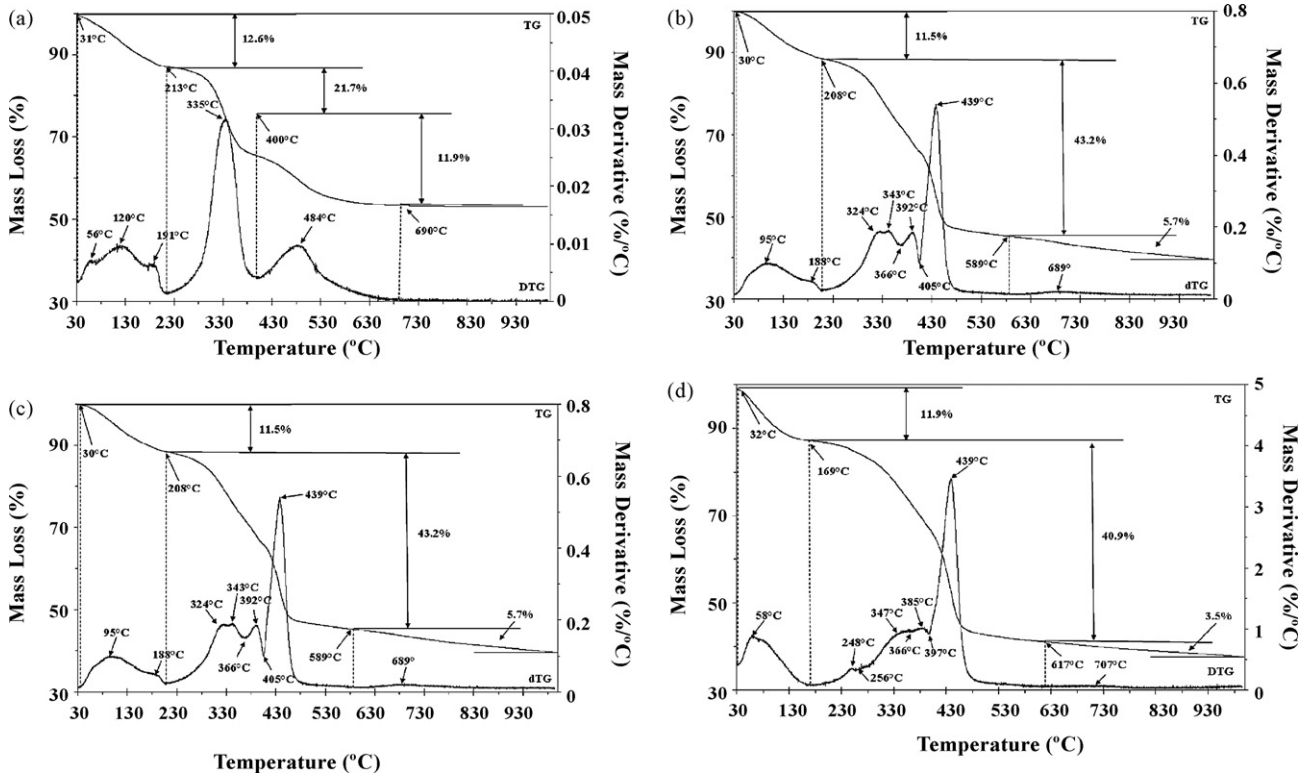

Fig. 6. Thermal gravimetric analyses curves of the resultants and surfactant: (a) LDH, (b) SDS, (c) LDH-S and (d) LDH-G.

has demonstrated that the frequencies of the asymmetric and symmetric $-CH_2$ stretching absorption bands are sensitive to the conformation of the intercalated surfactants within the clay interlayer space [46,47]. In the case of LDH-S, the asymmetric and symmetric CH_2 stretching absorption bands are located at 2918 and 2851 cm^{-1}, respectively. This suggests that the all-*trans* conformations are dominant for the alkyl chain of the intercalated surfactant [46,47]. However, for LDH-G, the asymmetric and symmetric CH_2 stretching absorption bands are located at 2923 and 2853 cm^{-1}, respectively, indicating that the conformation of the alkyl chain of the intercalated surfactant changes from all-*trans* to gauche [47]. This gives an important evidence for the successful grafting of the silane onto the LDH. When silane grafted onto LDH surfaces, strong covalent bonds between silane and LDH were formed. The bounded silane will occupy the space within the LDH interlayer space and hinder the intercalated surfactants having a regular arrangement. In other words, the intercalated surfactants are poorly ordered in LDH-G that those in LDH-S. Accordingly, the conformation of the alkyl chain of the intercalated surfactant changes from all-*trans* in LDH-S to gauche in LDH-G.

3.3. Thermal analysis

The thermogravimetric analysis results of all samples are shown in Fig. 6. The corresponding differential thermogravimetric analysis profiles are also shown for comparison. The LDH shows three mass loss steps. The first stage is from 31 to 213 °C with a total mass loss of 12.6%, attributed to the loss of adsorbed water, interlayer water and CO_3^{2-} absorbed on the surface. The dehydroxylation stage and partial loss of CO_3^{2-} begins at 213 °C and ends at 400 °C, with a mass loss of 21.7%. The last stage occurs from 400 to 690 °C with a mass loss of 11.9%, due to the completely loss of the interlayer anions to form layered double oxides (LDO) (mixed metallic oxides). The total mass loss observed is 46.1%.

The water loss stage of the LDH-S (Fig. 6c, 30–208 °C) is similar to that of LDH. The slight decrease in mass loss (11.3%) shows the less absorbed water molecules in the plate surfaces and interlayer spaces. This is due to the modification of LDH with SDS resulting in a change of the surface property of LDH from hydrophilicity to hydrophobicity as discussed in FTIR parts. A mass loss of ca. 22.6% is recorded at 208–405 °C in the TG curve of LDH-S, corresponding to the dehydroxylation. Here, it can be found that the content of –OH in LDH and LDH-S is similar. This reflects that the intercalation of SDS has no influence on the concentration of –OH on the LDH surfaces. A sharp peak at 405–589 °C in DTG curve of LDH-S is recorded, corresponding to a quick and large mass loss. As can be seen from Fig. 6b, within this temperature region (375–492 °C), SDS loses its alkyl chain (42.2%) [39]. Hence, we attribute this stage in LDH-S to loss both alkyl chain and residue CO_3^{2-}. Above 589 °C, LDH-S loss about 5.7% mass due to volatilization of $-OSO_2$ and further dehydroxylation. These procedures were evidenced in details by Clearfield and co-workers using FTIR spectra of samples after being calcinated to detect the evolved gases [39].

When the organosilane is bonded to the LDH surfaces, the thermal decomposition (Fig. 6c) shows significant differences when compared with LDH and LDH-S. Firstly, the mass loss due to the interlayer water disappeared, implying the water consumption during grafting reaction. The most important difference is that there is only 15.0% mass loss can be recorded in the process of dehydroxylation (169–397 °C). The much less content of –OH groups indicating the consumption of –OH groups when –Si–OH condensates with the LDH surface to form –Si–O–M (M = Mg^{2+} or Al^{3+}) as presumed from the changes of FTIR bands. In addition, decomposition of alkyl chain and volatilize interlayered anions procedure changes to 397–617 °C. The last mass loss at 617–790 °C is assigned to the layer collapse with loss of OH and SO_2 and formation of spinels.

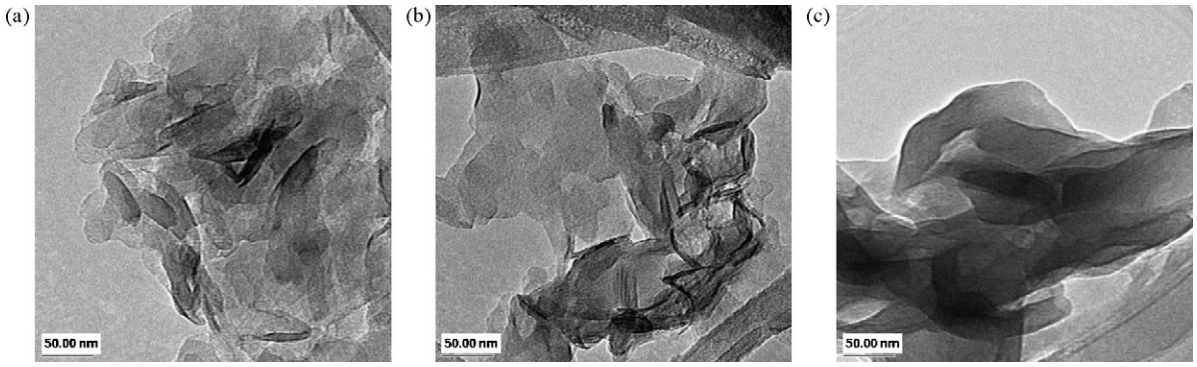

Fig. 7. TEM micrographs of (a) LDH, (b) LDH-S and (c) LDH-G.

3.4. TEM images

In order to find further evidences of the successful grafting of silane onto layered double hydroxide, the as-synthesized products were investigated using transmission electron microscopy. The obtained TEM images are displayed in Fig. 7. The nano-scale crystal particles with irregular shapes are observed in the image of LDH (Fig. 7a). The surfactant intercalated samples show rather different morphology (Fig. 7b). A combination of exfoliated layer and crystal particles are observed. The enlarged interlayers can be clearly seen in this image. The distance between two layers ranges from 2.5 to 5.0 nm, which is proved by the intense and board diffraction peaks in XRD pattern at low angle region. The grafted sample presents a distinct structure (Fig. 7c). The particles which are common in LDH are not observed after grafting. The single layers in a exfoliated state appear ribbon-like ultrathin sheets. It is suggested that a process of dissolution–precipitation–crystallisation is taking place. The layer is too thin and it gets curled when touched by high energy electrical beams, hence it is hard to accurately measure its lateral thickness. The measured value is 2.5 nm taking into account any error from the TEM technique itself.

4. Conclusions

The APTS-grafted LDHs have been synthesized via an in situ coprecipitation method. The resultant materials show a ribbon-like thin sheet in the TEM images with the lateral thickness estimated as 2.5 nm, demonstrating that the structure and morphology of the silane-grafted LDH is very different from the original LDH and anionic surfactant modified LDH. The occurrence of Si–O–M (M = Mg and Al) vibration at 996 cm^{-1} in the FTIR of the silylated LDH is an important evidence that suggests the APTS has been successfully grafted onto LDH. The conformation change of the intercalated surfactant from all-*trans* (LDH-S) to gauche (LDH-G) provides a complementary support for the success of the silane grafting. Meanwhile, less –OH concentration and interlayer water molecule in silane-grafted LDH as indicated by the TG curves suggests the –OH consumption during the condensation reaction between Si–OH and –OH on LDH surface. The present study shows that a kind of novel clay-based nanomaterials can be synthesized by grafting silane onto hydrotalcites. These nanomaterials are of potential applications in a lot of industrial fields including clay-based nanocomposites, adsorbents for removal of organic contaminants from water, flame retarding materials and layered double hydroxides polymer nanocomposites [22,48,49].

Acknowledgements

The financial and infra-structure supports of the National Natural Science Foundation of China (Grant No. 40572023) and National Science Fund for Distinguished Young Scholars (Grant No. 40725006) are acknowledged. The financial and infra-structure support of the Queensland University of Technology Inorganic Materials Research Program of the School of Physical and Chemical Sciences is gratefully acknowledged. The Australian Research Council (ARC) is thanked for funding. Qi Tao is grateful to The China Scholarship Council for the overseas funding to visit QUT.

References

[1] M.D.K. Ingall, C.H. Honeyman, J.V. Mercure, P.A. Bianconi, R.R. Kunz, J. Am. Chem. Soc. 121 (1999) 3607–3613.
[2] S. Angloher, J. Kecht, T. Bein, Chem. Mater. 19 (2007) 5797–5802.
[3] Y.R. Yeon, Y.J. Park, J.S. Lee, J.W. Park, S.G. Kang, C.H. Jun, Angew. Chem. Int. Ed. 47 (2008) 109–112.
[4] S. Oh, T. Kang, H. Kim, J. Moon, S. Hong, J. Yi, J. Membr. Sci. 301 (2007) 118–125.
[5] H. Lee, S.M. Dellatore, W.M. Miller, P.B. Messersmith, Science 318 (2007) 426–430.
[6] J.X. Zhu, P. Yuan, H.P. He, R. Frost, Q. Tao, W. Shen, T. Bostrom, J. Colloid Interface Sci. 319 (2008) 498–504.
[7] F. Cavani, F. Trifiro, A. Vaccari, Catal. Today 11 (1991) 173–301.
[8] N.D. Hutson, S.A. Speakman, E.A. Payzant, Chem. Mater. 16 (2004) 4135–4143.
[9] E.D. Dimotakis, T.J. Pinnavaia, Inorg. Chem. 29 (1990) 2393–2394.
[10] Y.W. You, H.T. Zhao, G.F. Vance, J. Mater. Chem. 12 (2002) 907–912.
[11] C. Domingo, E. Loste, J. Fraile, J. Supercrit. Fluids 37 (2006) 72–86.
[12] B.M. Choudary, N.S. Chowdari, K. Jyothi, M.L. Kantam, J. Am. Chem. Soc. 124 (2002) 5341–5349.
[13] M.C. Hermosin, I. Pavlovic, M.A. Ulibarri, J. Cornejo, Water Res. 30 (1996) 171–177.
[14] R.L. Frost, E. Mendelovici, J. Colloid Interface Sci. 294 (2006) 47–52.
[15] E. Mendelovici, R.L. Frost, J. Colloid Interface Sci. 289 (2005) 597–599.
[16] E. Mendelovici, R.L. Frost, J.T. Kloprogge, J. Colloid Interface Sci. 238 (2001) 273–278.
[17] G.G.C. Arizaga, A.S. Mangrich, J.E.F. da Costa Gardolinski, F. Wypych, J. Colloid Interface Sci. 320 (2008) 168–176.
[18] J.L. Guimaras, R. Marangoni, L.P. Ramos, F. Wypych, J. Colloid Interface Sci. 227 (2000) 445–451.
[19] F. Malherbe, J.-P. Besse, J. Solid State Chem. 155 (2000) 332–341.
[20] S. Nakagaki, F. Wypych, J. Colloid Interface Sci. 315 (2007) 142–157.
[21] N. Ukrainczyk, T. Matusinovic, S. Kurajica, B. Zimmermann, J. Sipusic, Thermochim. Acta 464 (2007) 7–15.
[22] F. Wypych, K.G. Satyanarayana, J. Colloid Interface Sci. 285 (2005) 532–543.
[23] A.Y. Park, H. Kwon, A.J. Woo, S.J. Kim, Adv. Mater. 17 (2005) 106–109.
[24] S. Nakagaki, M. Halma, A. Bail, G.G.C. Arizaga, F. Wypych, J. Colloid Interface Sci. 281 (2005) 417–423.
[25] C. Li, G. Wang, D.G. Evans, X. Duan, J. Solid State Chem. 177 (2004) 4569–4575.
[26] G. Kickelbick, Hybrid Materials: Synthesis, Characterization, and Applications, 1st ed., Wiley–VCH, 2007.
[27] R.Z. Ma, Z.P. Liu, L. Li, N. Iyi, T. Sasaki, J. Mater. Chem. 16 (2006) 3809–3813.
[28] M. Adachi-Pagano, C. Forano, J.P. Besse, Chem. Commun. (2000) 91–92.
[29] T. Hibino, W. Jones, J. Mater. Chem. 11 (2001) 1321–1323.
[30] F. Leroux, M. Adachi-Pagano, M. Intissar, S. Chauviere, C. Forano, J.P. Besse, J. Mater. Chem. 11 (2001) 105–112.
[31] S. Miyata, T. Kumura, M. Shimada, Kompositionsmetallhydroxyde und Verfahren zuderen Herstellung. German, 2,061,156.
[32] S. Miyata, Clays Clay Miner. 23 (1975) 369–375.
[33] H. Zhao, K.L. Nagy, J. Colloid Interface Sci. 274 (2004) 613–624.
[34] G.A. Bubniak, W.H. Schreiner, N. Mattoso, F. Wypych, Langmuir 18 (2002) 5967–5970.
[35] J.X. Zhu, H.P. He, J.G. Guo, D. Yang, X.D. Xie, Chin. Sci. Bull. 48 (2003) 368–372.
[36] J.L. Bonczek, W.G. Harris, P. Nkedi-Kizza, Clays Clay Miner. 50 (2002) 11–17.
[37] G. Lagaly, Clay Miner. 16 (1981) 1–21.

[38] H.P. He, R.L. Frost, F. Deng, J.X. Zhu, X.Y. Wen, P. Yuan, Clays Clay Miner. 52 (2004) 350–356.
[39] A. Clearfield, M. Kieke, J. Kwan, J.L. Colon, R.C. Wang, J. Incl. Phenom. Macrocyclic Chem. 11 (1991) 361–378.
[40] Q. Tao, Y.M. Zhang, X. Zhang, P. Yuan, H.P. He, J. Solid State Chem. 179 (2006) 708–715.
[41] A.K. Chauhan, D.K. Aswal, S.P. Koiry, S.K. Gupta, J.V. Yakhmi, C. Surgers, D. Guerin, S. Lenfant, D. Vuillaume, Appl. Phys. A: Mater. Sci. Process. 90 (2008) 581–589.
[42] H.N. Negrete, J.M. Letoffe, J.L. Putaux, L. David, E. Bourgeat-Lami, Langmuir 20 (2004) 1564–1571.
[43] Z.P. Liu, R.Z. Ma, M. Osada, N. Iyi, Y. Ebina, K. Takada, T. Sasaki, J. Am. Chem. Soc. 128 (2006) 4872–4880.
[44] J.T. Kloprogge, L. Hickey, R.L. Frost, J. Raman Spectrosc. 35 (2004) 967–974.
[45] R. Pena-Alonso, F. Rubio, J. Rubio, J.L. Oteo, J. Mater. Sci. 42 (2007) 595–603.
[46] H. He, R.L. Frost, J. Zhu, Spectrochim. Acta Part A: Mol. Biomol. Spectrosc. 60 (2004) 2853–2859.
[47] R.A. Vaia, R.K. Teukolsky, E.P. Giannelis, Chem. Mater. 6 (1994) 1017–1022.
[48] W. Chen, B.J. Qu, Chin. J. Chem. 21 (2003) 998–1000.
[49] S. O'Leary, D. O'Hare, G. Seeley, Chem. Commun. (2002) 1506–1507.